Received: 11 April 2022 | Accepted: 3 May 2022

DOI: 10.1002/prp2.978

ORIGINAL ARTICLE

Exploring the kinetic selectivity of drugs targeting the β_1-adrenoceptor

David A. Sykes[1,2] | Mireia Jiménez-Rosés[1,2] | John Reilly[3] | Robin A. Fairhurst[3] | Steven J. Charlton[1,2] | Dmitry B. Veprintsev[1,2]

[1]Centre of Membrane Proteins and Receptors (COMPARE), University of Nottingham, Midlands, UK

[2]Division of Physiology, Pharmacology & Neuroscience, School of Life Sciences, University of Nottingham, Nottingham, UK

[3]Novartis Institutes for BioMedical Research, Basel, Switzerland

Correspondence
David A. Sykes, Steven J. Charlton and Dmitry B. Veprintsev, School of Life Sciences, Queen's Medical Centre, University of Nottingham, Nottingham NG7 2UH, UK.
Email: david.sykes@nottingham.ac.uk; steven.charlton@nottingham.ac.uk; dmitry.veprintsev@nottingham.ac.uk

Funding information
Novartis Institutes for Biomedical Research

Abstract

In this study, we report the β_1-adrenoceptor binding kinetics of several clinically relevant $\beta_{1/2}$-adrenoceptor ($\beta_{1/2}$AR) agonists and antagonists. [^{3}H]-DHA was used to label CHO-β_1AR for binding studies. The kinetics of ligand binding was assessed using a competition association binding method. Ligand physicochemical properties, including $\log D_{7.4}$ and the immobilized artificial membrane partition coefficient (K_{IAM}), were assessed using column-based methods. Protein Data Bank (PDB) structures and hydrophobic and electrostatic surface maps were constructed in PyMOL. We demonstrate that the hydrophobic properties of a molecule directly affect its kinetic association rate (k_{on}) and affinity for the β_1AR. In contrast to our findings at the β_2-adrenoceptor, K_{IAM}, reflecting both hydrophobic and electrostatic interactions of the drug with the charged surface of biological membranes, was no better predictor than simple hydrophobicity measurements such as clogP or $\log D_{7.4}$, at predicting association rate. Bisoprolol proved kinetically selective for the β_1AR subtype, dissociating 50 times slower and partly explaining its higher measured affinity for the β_1AR. We speculate that the association of positively charged ligands at the β_1AR is curtailed somewhat by its predominantly neutral/positive charged extracellular surface. Consequently, hydrophobic interactions in the ligand-binding pocket dominate the kinetics of ligand binding. In comparison at the β_2AR, a combination of hydrophobicity and negative charge attracts basic, positively charged ligands to the receptor's surface promoting the kinetics of ligand binding. Additionally, we reveal the potential role kinetics plays in the on-target and off-target pharmacology of clinically used β-blockers.

KEYWORDS
adrenergic, beta-blockers, kinetic selectivity, physicochemical properties

Abbreviations: [^{3}H]-DHA, 1-[4,6-propyl-3H] dihydroalprenolol; B_{max}, maximum number of binding sites; c.p.m., counts per minute; CHO, Chinese hamster ovary; DOA, duration of action; GTP, guanosine-5′-triphosphate; HBSS, Hanks' balanced salt solution; IAM, immobilized artificial membrane; MD, molecular dynamic; NSB, non-specific binding; PDB, Protein Data Bank.

1 | INTRODUCTION

The β_1-adrenergic receptor is involved in the sympathetic nervous systems control of the circulation mainly via its stimulatory signaling effects on the heart. So called β-blockers, also known as β-adrenergic receptor blockers, decrease heart rate and blood pressure through their actions at β_1-adrenoceptors and are, therefore, useful in the treatment of hypertension and heart failure. The promiscuous binding of β-adrenergic ligands to the closely related subtypes of the β-adrenoceptor (e.g., the β_2-adrenergic receptor) leads to commonly observed side effects such as fatigue, decreased peripheral circulation, and increased airway resistance. This cross-reactivity has long been considered a risk factor in asthmatic patients, with deaths attributed to β-blockers use in the very early years of their use, leading to the recommendation that non-selective β-blockers be avoided in asthmatic subjects.[1,2] Due to their high sequence and structural similarity, the molecular basis of ligand selectivity between the β-adrenergic receptor subtypes remains to be fully understood. This has led to the suggestion that the kinetic process of ligand binding itself may contribute to ligand specificity for individual receptor subtypes. Although the process of ligand binding is not possible to study using direct structural methods, molecular dynamics (MD) studies have shed some light on the molecular basis of receptor selectivity and even on the pathway of ligand binding and dissociation.[3-5] Kinetic selectivity has been shown to be an important factor in dictating the therapeutic action of muscarinic M_3 antagonists which target the lung to treat chronic obstructive pulmonary disease or COPD.[6,7] Here a longer residency time at the muscarinic M_3 receptor over the M_2 receptor subtype is favored from a therapeutic perspective helping to relax smooth muscle cells and open the airways, avoiding off-target cardiac effects. In direct contrast, the relevance of kinetic selectivity in the therapeutic action of β-blockers remains unexplored, largely due to a lack of information on the binding kinetics of these ligands at the β_1-adrenoceptor.

The kinetics of synthetic and endogenous agonists and antagonists at the β_1AR have been studied in the past albeit at room temperature reducing their physiological significance.[8-10] The aim of this work was to determine the kinetics of a series of well-described β_1-adrenoceptor antagonists and agonists and several clinically relevant β_1-adrenoceptor antagonists at the physiological temperature (37°C).

A secondary aim was to determine if kinetic selectivity has any role to play in the known side effect profile of these widely prescribed compounds. Our previous studies of β_2-adrenergic receptor kinetics highlighted the importance of "membrane-like" polar and hydrophobic interactions in driving ligand binding through changes in ligand association rate (or k_{on}).[11,12] A more detailed understanding of the molecular basis of $\beta_{1/2}$-adrenergic receptor antagonist selectivity is likely to provide a novel rationale for the discovery of more selective ligands, which target the heart with potentially fewer side effects.

2 | MATERIALS AND METHODS

[^{3}H]-DHA (1-[4,6-propyl-^{3}H]dihydroalprenolol, specific activity 91 Ci mmol^{-1}) was obtained from PerkinElmer Life and Analytical Sciences. Ninety-six deep well plates and 500 cm^2 cell culture plates were purchased from Fisher Scientific. Millipore 96-well GF/B filter plates were purchased from Receptor Technologies. Sodium bicarbonate, HEPES, Hank Balanced Salts, ascorbic acid, EDTA, sodium chloride, GTP, bisoprolol hemifumarate, (S)-(−) atenolol, labetalol hydrochloride, (±) metoprolol, carvedilol, (S)-(−) propranolol hydrochloride, salmeterol xinafoate, ICI 118551 hydrochloride, (±) sotalol hydrochloride, nadolol, (S)-(−) cyanopindolol hemifumarate, formoterol fumarate, and CGP-20712A methanesulfonate were obtained from Sigma Chemical Co Ltd. Bucindolol, (S)-timolol maleate and CGP12177 hydrochloride were obtained from Tocris Cookson, Inc. Hanks' balanced salt solution (HBSS) was prepared according to the manufacturer's instructions and consists of the following: calcium chloride 1.3 mM, magnesium sulfate 0.8 mM, potassium chloride 5.4 mM, potassium phosphate monobasic 0.4 mM, sodium chloride 137 mM, sodium phosphate dibasic 0.3 mM, D-Glucose 5.6 mM, and sodium bicarbonate 4.2 mM. All cell culture reagents were purchased from Gibco (Invitrogen).

2.1 | Cell culture and membrane preparation

CHO cells stably transfected with the human β_1-adrenoceptor were grown adherently in Ham's F-12 Nutrient Mix GlutaMAX-1, containing 10% fetal calf serum, and 0.5 mg·mL^{-1} Geneticin (G-418). Cells were maintained at 37°C in 5% CO_2/humidified air and routinely subcultured at a ratio between 1:10 and 1:20 twice weekly using trypsin–EDTA to lift cells. Cell membranes were prepared and stored as described previously.[11]

2.2 | Common procedures applicable to all radioligand binding experiments

All radioligand binding experiments using 1-[4,6-propyl-^{3}H]dihydroalprenolol ([^{3}H]-DHA specific activity 91 Ci·mmol^{-1}) were conducted in 96 deep-well plates, in assay binding buffer, HBSS pH 7.4, 0.01% ascorbic acid, and 100 μM GTP. GTP was included to remove the G protein-coupled population of receptors which can result in two binding sites in membrane preparations because the Motulsky and Mahan model is only appropriate for ligands competing at a single site. In all cases, non-specific binding (NSB) was determined in the presence of 1 μM propranolol. After the indicated incubation period, bound and free radiolabels were separated by rapid vacuum filtration using a FilterMate™ Cell Harvester (PerkinElmer Life and Analytical Sciences) onto 96-well GF/B filter plates (Millipore) previously coated with 0.5% (w/v) polyethylenimine and rapidly washed three times with 1 ml

of ice-cold 75 mM HEPES, pH 7.4. After drying (>4 h), 40 ml of Microscint™ 20 (PerkinElmer Life and Analytical Sciences) was added to each well and radioactivity was quantified using single-photon counting on a TopCount™ microplate scintillation counter (PerkinElmer Life and Analytical Sciences). Aliquots of radiolabel were also quantified accurately to determine how much radioactivity was added to each well using liquid scintillation spectrometry on LS 6500 scintillation counter (Beckman Coulter). In all experiments, total binding never exceeded more than 10% of that added, limiting complications associated with depletion of the free radioligand concentration.[13]

2.3 | Saturation binding studies

CHO cell membranes containing the β_1-adrenoceptor were incubated in 96-deep well plates at 37°C in assay binding buffer with a range of concentrations of [^{3}H]-DHA (~12–0.01 nM) at 30 μg per well, for 180 min with gentle agitation to ensure equilibrium was reached prior to filtering. Saturation binding was performed in a final assay volume of to 1.5 ml to avoid significant ligand depletion.

2.4 | Determination of the association rate (k_{on}) and dissociation rate (k_{off}) of [^{3}H]-DHA

To accurately determine k_{on} and k_{off} values, the observed rate of association (k_{ob}) was calculated using at least three different concentrations of [^{3}H]-DHA. The appropriate concentration of radioligand was incubated with β_1-adrenoceptor CHO cell membranes (30 μg·per well) in assay binding buffer with gentle agitation (final assay volume 0.5 ml. Exact concentrations were calculated in each experiment by liquid scintillation counting. Free radioligand was separated by rapid filtration at multiple time points to construct association kinetic curves as described previously by Sykes & Charlton.[11] The resulting data were globally fitted to the association kinetic model (Equation 2) to derive a single best fit estimate for k_{on} and k_{off} as described under Data analysis.

2.5 | Determination of affinity constants (K_i)

To obtain affinity estimates of unlabelled ligand, [^{3}H]-DHA competition experiments were performed at equilibrium. [^{3}H]-DHA was used at a concentration of approximately 3 nM (final assay volume of 0.5 ml), such that the total binding never exceeded more than 10% of that added. Radioligand was incubated in the presence of the indicated concentration of unlabelled ligand (10 concentrations in total) and CHO cell membranes (30 μg per well) at 37°C, with gentle agitation for 180 min prior to filtering.

2.6 | Competition binding kinetics

The kinetic parameters of unlabelled ligand were assessed using a competition kinetic binding assay originally described by Motulsky & Mahan[14] and developed for the β_1-adrenoceptor by Sykes & Charlton.[11] This approach involves the simultaneous addition of both radioligand and competitor to receptor preparation, so that at $t = 0$ all receptors are unoccupied.

Approximately 3 nM [^{3}H]-DHA (a concentration which avoids ligand depletion in this assay volume) was added simultaneously with the unlabelled compound (at $t = 0$) to CHO cell membranes containing the human β_1-adrenoceptor (30 μg· per well) in 0.5 m assay buffer. The degree of [^{3}H]-DHA bound to the receptor was assessed at several time points by filtration harvesting and liquid scintillation counting, as described previously. NSB was determined as the amount of radioactivity bound to the filters and membrane in the presence of propranolol (1 μM) and was subtracted from each time point, meaning that $t = 0$ was always equal to zero. Each time point was conducted on the same 96-deep well plate incubated at 37°C with constant agitation. Reactions were considered stopped once the membranes reached the filter, and the first wash was applied within 1 s. A single concentration of unlabeled competitor was tested, as rate parameters were shown to be independent of unlabeled ligand concentration (data not shown). All compounds were tested at either 1-, 3-, 10- or 100-fold their respective K_i and data were globally fitted using Equation 4 to simultaneously calculate k_{on} and k_{off}. For rapidly and slowly dissociating compounds the first time point studied was within 5 seconds of membrane addition, a key factor in the successful determination of the kinetics of the most rapidly dissociating compounds.

Different ligand concentrations were chosen as compounds with a long residence time equilibrate more slowly so a higher relative concentration is required to ensure the experiments reach equilibrium within a reasonable time frame (90 min), while still maintaining a good signal to noise. The actual concentrations used were selected from a preliminary experiment using three different concentrations of each ligand (data not shown).

2.7 | LogD$_{7.4}$ and immobilized artificial membrane chromatography

All HPLC experiments were carried out as previously described by Sykes et al.[12]

2.8 | Data analysis and statistical procedures

As the amount of radioactivity varied slightly for each experiment (<5%), data are shown graphically as the mean ± range for individual representative experiments, whereas all values reported in the

text and tables are mean ± SEM for the indicated number of experiments unless otherwise stated. All experiments were analyzed by either Deming regression or non-linear regression using Prism 8.0 (GraphPad Software).

2.8.1 | Competition binding

Competition displacement binding data were fitted to sigmoidal (variable slope) curves using a four-parameter logistic equation:

$$Y = \text{Bottom} + (\text{Top} - \text{Bottom})\left(1 + 10\left[\log \text{IC}_{50} - X\right] \cdot \text{HillSlope}\right) \quad (1)$$

IC_{50} values obtained from the inhibition curves were converted to K_i values using the method of Cheng and Prusoff.[15]

2.8.2 | Association binding

[^{3}H]-DHA association data were globally fitted to Equation 2, where L is the concentration of radioligand in nM using GraphPad Prism 8.0 to determine a best fit estimate for k_{on} and k_{off}.

$$k_{ob} = [L] \cdot k_{on} + k_{off} \quad (2)$$

In addition, the same data were analyzed using nonlinear regression to fit the specific binding data to the one-phase exponential association equation:

$$Y = Y_{max} \times \left[1 - \exp(-k_{ob} \times X)\right] \quad (3)$$

where X is time and the observed rate constant, k_{ob}, is expressed in units of inverse time, min^{-1}. Concentration of the radioligand was plotted against k_{ob} to allow estimation of kinetic parameters through linear regression. The slope of the line being equivalent to k_{on} and the Y intercept, when X = zero being equivalent to k_{off}.

2.8.3 | Competition kinetic binding

Association and dissociation rates for unlabelled agonists were calculated using the equations described by Motulsky and Mahan[14] using a global fitting model:

$$K_A = k_1[L] + k_2$$

$$K_B = k_3[I] + k_4$$

$$S = \sqrt{\left((K_A - K_A)\right)^2 + 4 \bullet k_1 \bullet k_3 \bullet L \bullet I \bullet 10^{-18}}$$

$$K_F = 0.5 \times (K_A + K_B + S)$$
$$K_S = 0.5 \times (K_A + K_B - S)$$

$$Q = \frac{B_{max} \times K_1 \times L \times 10^{-9}}{K_F - K_S}$$

$$Y = Q \cdot \left(\frac{k_4 \cdot (K_F - K_S)}{K_F \cdot K_S} + \frac{k_4 - K_F}{K_F} \exp^{(-K_F \cdot X)} - \frac{k_4 K_S}{K_S} \exp^{(-K_S \cdot X)}\right) \quad (4)$$

where X is time (min), Y is specific binding (c.p.m.), $k1$ is k_{on} of the tracer [^{3}H]-DHA, $k2$ is k_{off} of the tracer [^{3}H]-DHA, L is the concentration of [^{3}H]-DHA used (nM), and I is the concentration of unlabeled ligand (nM). Fixing the above parameters allowed the following to be simultaneously calculated: B_{max} is total binding (c.p.m.), $k3$ is association rate of unlabeled ligand (M^{-1} min^{-1}) or k_{on}, and $k4$ is the dissociation rate of unlabelled ligand (min^{-1}) or k_{off}.

2.8.4 | Linear correlations

The correlation between datasets was determined by calculating a Pearson correlation coefficient (presented as r^2 the coefficient of determination, which shows percentage variation in y which is explained by all the x variables together) in GraphPad Prism 8.0.

2.9 | Protein Data Bank structures and hydrophobic and electrostatic surface maps

The crystal structures of the β_1AR[10] and β_2AR[16] were obtained from the PDB (PDB entries 7BVQ and 5JQH, respectively). The hydrophobic surface map was obtained using a modified version (changing the scale of colors to purple and yellow) of color_h.py script (pymolwiki.org/index.php/Color_h) using PyMOL. For production of the electrostatic surface map, we used the PyMOL APBS electrostatic plugin using the default parameters (changing the scale colors to blue and red only) (MG Lerner and HA Carlos. APBS plugin for PyMOL, 2006, University of Michigan).

3 | RESULTS

3.1 | Equilibrium and kinetic binding parameters for β_1-adrenoceptor ligands

Initially, the binding affinity of the radioligand [^{3}H]-DHA for the β_1-adrenoceptor (shown in Figure 1A) was measured at equilibrium in HBSS containing GTP (100 μM) at 37°C. GTP was included to ensure that agonist binding only occurred to the uncoupled form of the receptor. Binding affinities (K_i values) for the β_1-adrenoceptor ligands determined in the presence to GTP are summarized in Table 1 and associated curves are presented in Figure 1B–D. To determine the association and dissociation rates of the β_1-adrenoceptor ligands, we utilized a competition kinetic radioligand binding assay as previously described by Sykes & Charlton.[11] Firstly, we characterized the binding kinetics of the radiolabelled ligand [^{3}H]-DHA by monitoring

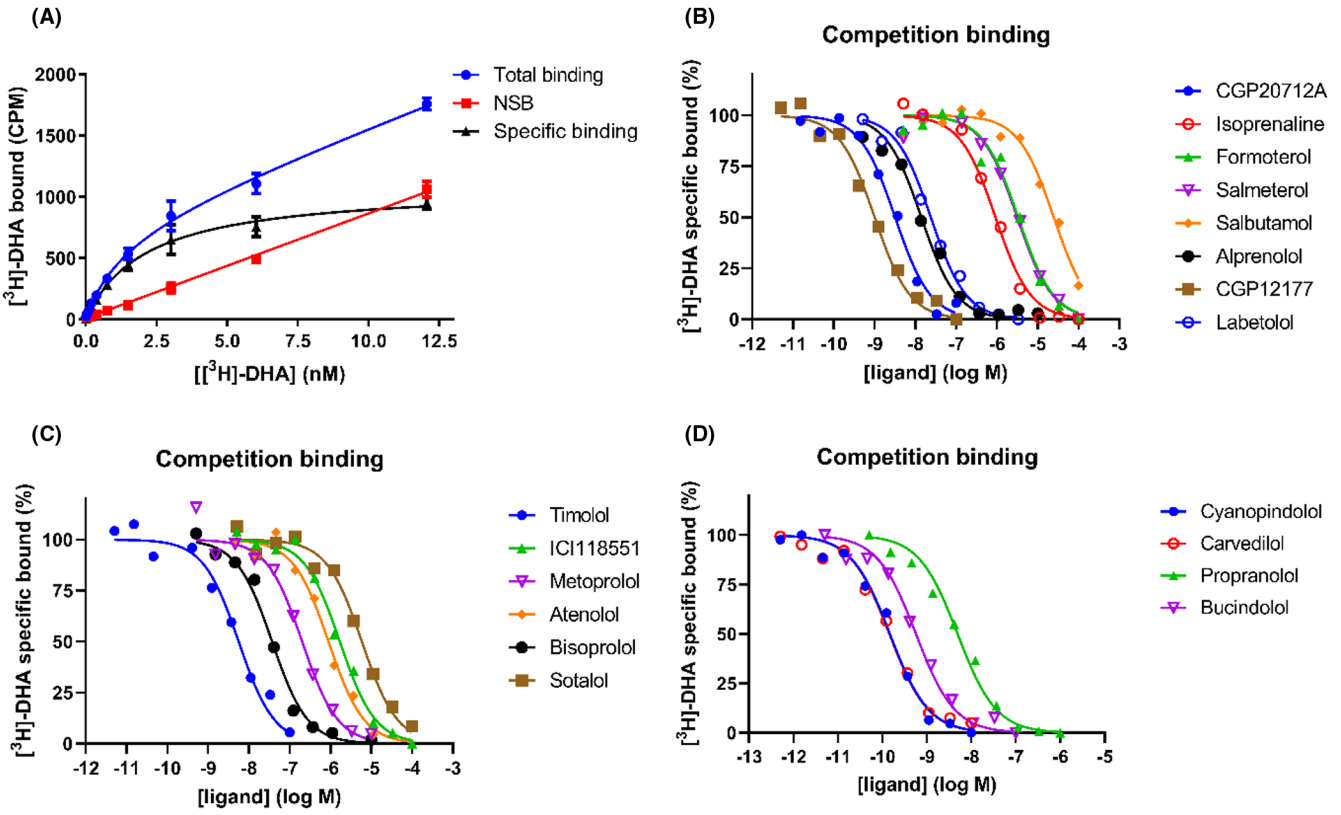

FIGURE 1 [^{3}H]-DHA saturation binding plus competition binding between [^{3}H]-DHA and β-adrenergic ligands for human β_1-adrenoceptors expressed in the CHO cells in the presence of GTP. (A) [^{3}H]-DHA saturation binding, Membranes (30 μg per well) from CHO-β_1 cells were incubated in HBSS containing 0.1 mM GTP (as described in Methods) and increasing concentrations of radioligand for 180 min at 37°C with gentle agitation. Displacement of [^{3}H]-DHA (3 nM) by increasing concentrations of (B) CGP20712A, isoprenaline, formoterol, salmeterol, salbutamol, alprenolol, CGP12177 and labetolol. (C) timolol, ICI 118551, metoprolol, atenolol, bisoprolol, sotalol. (D) (S)-cyanopindolol, carvedilol, propranolol and bucindolol. NSB was defined by 1 μM propranolol. Data are presented as the mean ± range from a representative of three experiments performed in singlet.

the observed association rates at 3 different ligand concentrations (Figure 2A). The observed rate of association, calculated using Equation 3, and was related to [^{3}H]-DHA concentration in a linear fashion (Figure 2B). Kinetic rate parameters for [^{3}H]-DHA were calculated by globally fitting the association time courses, resulting in a k_{on} of $5.28 \pm 0.48 \times 10^8$ M^{-1} min^{-1} and a k_{off} of 0.46 ± 0.03 min^{-1} ($K_d = 0.94 \pm 17$ nM).

Representative kinetic competition curves for selected β-adrenoceptor ligands are shown in Figure 3A–H. Progression curves for [^{3}H]-DHA alone and in the presence of competitor were globally fitted to Equation 4 enabling the calculation of both k_{on} (*k*3) and k_{off} (*k*4) for each of the ligands, as reported in Table 1. There was a very wide range in dissociation rates for the different ligands, with drug-target residency times ($1/k_{off}$) ranging between 0.07 min for the rapidly dissociating salmeterol to 66.67 min for cyanopindolol. To validate the rate constants, the kinetically derived K_d values (k_{off}/k_{on}) were compared with the inhibitory constant (K_i) obtained from equilibrium competition binding experiments (Figure S1). There was a very good correlation ($r^2 = 0.97$, $p < 0.0001$) between these two values, indicating the kinetics parameters were consistent with the equilibrium inhibitory constant.

3.2 | Measurements of lipophilicity and membrane interactions

The degree of membrane interaction, denoted K_{IAM}, assessed using a chromatographic method and calculated logP (clogP) values and the measured partition coefficient $logD_{7.4}$ are detailed in.[12] Drug membrane interaction is assessed using a chromatographic method that uses immobilized artificial membranes (IAMs) consisting of monolayers of phospholipid covalently immobilized on a silica surface, mimicking the lipid environment of a fluid cell membrane on a solid matrix.[12,17] Compounds with longer retention times on this column have higher affinity for phospholipids and will, therefore, theoretically have a higher calculated membrane partition coefficient, denoted K_{IAM}. The main difference between the $logD_{7.4}$ measure, that reflects hydrophobicity of the compound and IAM systems being the key role of electrostatics in the differential binding of the charged

TABLE 1 Kinetic binding parameters of unlabeled ligands for human β_1-adrenoceptor receptors

Ligand	k_{off} (min^{-1})	k_{on} (M^{-1} min^{-1})	Residence time (min)	pK_d	pK_i
Bisoprolol	0.14 ±0.06	1.96 ±0.26×10^7	7.14	8.20 ±0.13	7.86 ±0.11
Atenolol	6.19 ±2.38	4.03 ±1.29×10^7	0.16	6.84 ±0.04	6.59 ±0.22
Labetolol	1.74 ±0.55	2.85 ±0.91×10^8	0.57	8.21 ±0.07	8.01 ±0.12
Metoprolol	3.41 ±0.85	1.24 ±0.11×10^8	0.29	7.59 ±0.10	7.20 ±0.15
Bucindolol	0.11 ±0.02	1.11 ±0.25×10^9	9.09	10.00 ±0.04	9.57 ±0.11
Carvedilol	0.09 ±0.02	1.97 ±0.39×10^9	11.11	10.36 ±0.13	9.84 ±0.23
Propranolol	0.91 ±0.03	1.28 ±0.22×10^9	1.10	9.13 ±0.09	9.51 ±0.09
Salmeterol	14.3 ±3.65	2.63 ±0.21×10^7	0.07	6.29 ±0.08	5.92 ±0.05
ICI 118, 551	7.40 ±1.31	6.80 ±2.40×10^7	0.14	6.88 ±0.16	6.14 ±0.13
Sotalol	8.49 ±3.23	8.47 ±3.16×10^6	0.12	6.00 ±0.03	5.60 ±0.05
Nadolol	0.17 ±0.03	7.68 ±0.79×10^6	5.88	7.65 ±0.04	7.47 ±0.15
Formoterol	9.97 ±2.43	1.68 ±0.11×10^7	0.10	6.25 ±0.12	5.84 ±0.05
Timolol	0.05 ±0.01	9.66 ±2.42×10^7	20.00	9.24 ±0.06	8.75 ±0.05
Cyanopindolol	0.015 ±0.003	2.99 ±0.23×10^8	66.67	10.34 ±0.09	9.93 ±0.09
CGP12177	0.08 ±0.02	5.07 ±0.93×10^8	12.50	9.83 ±0.11	9.50 ±0.22
Isoprenaline	4.77 ±1.74	2.51 ±0.44×10^7	0.21	6.78 ±0.16	6.49 ±0.09
Salbutamol	9.81 ±2.60	1.96 ±0.77×10^7	0.10	4.91 ±0.02	5.27 ±0.11
CGP20712A	0.22 ±0.03	4.14 ±0.60×10^8	4.55	9.27 ±0.08	8.75 ±0.06

Note: Data are mean ± SEM for ≥3 experiments performed in singlet.

ligands to the anisotropic IAM column,[18] mimicking the effects seen in biological membranes.

3.3 | Relationship between kinetics and membrane interactions

The association rate parameter k_{on} is calculated from the observed on-rate (k_{obs}) which is highly dependent on drug concentration. We have demonstrated previously that drugs possessing high membrane affinity appear to have a more rapid association rate, potentially due to an increase in the local concentration of compound.[12,19]

The degree of membrane interaction is routinely assessed using a chromatographic method. The calculated membrane partition coefficient, denoted K_{IAM}, logP (clogP) and the measured partition coefficient $logD_{7.4}$ used in the following plots are detailed in.[12] Test compound Log $D_{7.4}$ values were significantly correlated (r^2 =0.32, p = 0.019) with k_{on} determined in the competition kinetic assay (Figure 4A), with lipophilic compounds having a faster association rate. A very similar correlation of k_{on} with $logK_{IAM}$ was observed (Figure 4B, r^2 =0.35, p = 0.013), suggesting that a simple isotropic, single-parameter model may be sufficient to describe the interaction of these drugs with the β_1-adrenoceptor. This was supported by comparisons between clogP and k_{on} which also showed a better correlation than observed with K_{IAM} (r^2 =0.48, p <0.002, data not shown). CGP20712A was excluded from these and subsequent analysis as no K_{IAM} data or corresponding β_2AR binding data was available.

The dissociation rate (or k_{off}) of a drug is not dependent upon drug concentration, so should be independent of the affinity of interaction with the membrane. Reassuringly, when the k_{off} for each compound was compared with either its $logD_{7.4}$ or $logK_{IAM}$ no correlation was observed (p >0.05, Figure 4C,D respectively).

The role of kinetics in dictating β_1-adrenoceptor compound affinity is presented in Figure 5A. Of the clinically used β-blockers under study, bisoprolol and nadolol stand out as possessing relatively slow on-rates in the region of ~10^7 M^{-1} min^{-1} and relatively slow off rates (~0.1 min^{-1}). In contrast other clinically used agents such as metoprolol and atenolol have much faster dissociation rates (3–10 min^{-1}) but higher relative association rates.

A comparison $\beta_{1/2}$-adrenoceptor compound dissociation and association kinetics is presented in Figure 5B,C. Of the clinically used β-blockers bisoprolol again stands out as the only truly β_1-adrenoceptor selective compound based on its kinetic affinity, a feature that is seemingly dictated by its dissociation rate from the β_1-adrenoceptor (see Figure 5B,D). The majority of ligands demonstrate a faster association rate at the β_2-adrenoceptor apart from the clinically used β-blocker atenolol (Figure 5C). Other key observations in terms of understanding β-adrenergic ligand selectivity are the pronounced reduction in the β_1-adrenoceptor association and dissociation rate of salmeterol relative to salbutamol when we compare kinetic values across the two receptors (Figure 5B,C). Similarly,

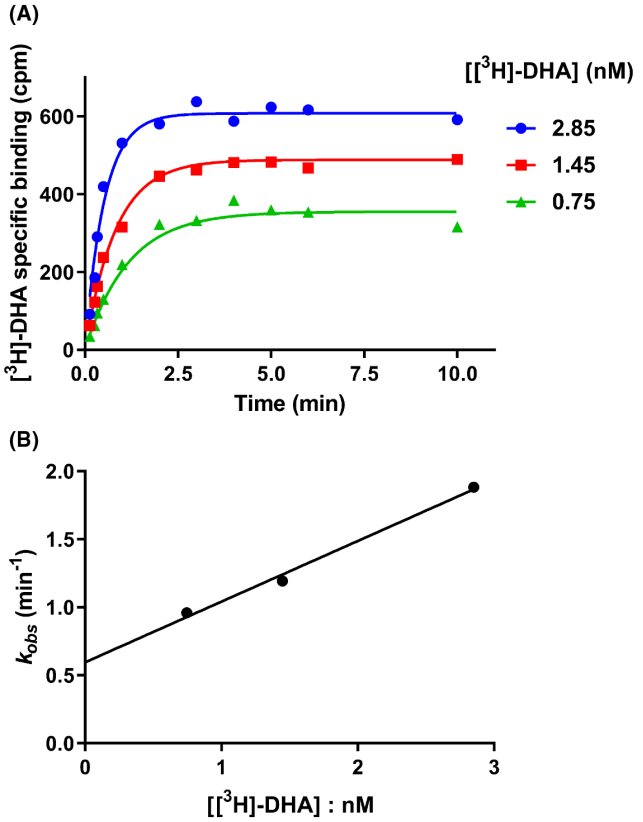

FIGURE 2 Determination of [^{3}H]-DHA kinetic binding parameters. (A) Observed association kinetics of the interaction of [^{3}H]-DHA with CHO membranes expressing the human β_1-adrenoceptors. (B) Plot of ligand concentration verses k_{ob}. Binding followed a simple law of mass action model, k_{ob} increasing in a linear manner with radioligand concentration. Data are presented as the mean ± range from a representative of three experiments performed in singlet.

the lower affinity of ICI 118551 for the β_1-adrenoceptor appears to be dictated by a combination of a reduced association and increased dissociation rate.

3.4 | Using kinetic parameters to model the rate of receptor occupancy and dissociation from the β_1 and β_2 adrenoceptors

The rate of receptor occupancy is one factor, which could potentially play a central role in the rate of onset of the actions of clinically used β-blockers. To investigate this, we stimulated their k_{obs} at the β_1 and β_2 adrenoceptors using a concentration 30× K_d their β_1-adrenoceptor affinity. Under these conditions there were clear differences in the rate of association of the four clinically used compounds with bisoprolol and carvedilol exhibiting a slower rate of $\beta_{1/2}$ receptor occupancy than the other clinically used ligands tested metoprolol and atenolol (Figure 6A–D) that saturated the receptors faster.

Another factor which could play a role in the duration of action (DOA) of clinically used β-blockers is their rates of dissociation from the β-adrenoceptors. In the simulations compound dissociation is initiated by the removal of free ligand at the 5 min mark. These simulations show that for atenolol and metoprolol receptor binding is fully reversed within 5 min, suggesting that dissociation rate has little or no role to play in the DOA of these two clinically used compounds (Figure 6B,D). Atenolol achieves a marginally lower level of occupancy at the β_2-adrenoceptors but its slower dissociation rate from this receptor equates to a marginally extended occupancy at this receptor.

In contrast, dissociation of bisoprolol is noticeably slower from the β_1-adrenoceptors compared to the β_2-adrenoceptor. And whilst full dissociation occurs from the β_2-adrenoceptor in a matter of seconds, it takes approximately 40 min for full dissociation from the β_1-adrenoceptor (Figure 6A). Carvedilol is a third-generation high-affinity β-blocker, and it is noticeable that it displays both higher affinity for the β_2-adrenoceptor and a much slower rate of dissociation, which leads to an extended occupancy at this receptor (Figure 6C). β_1-adrenoceptors residence time values from these simulations are detailed in Table 1. Residence time values for β_2-adrenoceptors were taken from a previous publication.[12]

4 | DISCUSSION

This study reports the kinetic rate constants of a number of β_1-adrenoceptor antagonists and agonists under physiological conditions allowing direct comparisons with earlier kinetic studies of the β_2-adrenoceptor.[11,12] Previous findings demonstrate how local drug concentrations near receptors embedded in biological membranes can directly influence their observed pharmacology.[12,19] Having established that a membrane bilayer acts as a medium by which drug molecules interact or locate low concentrations of a receptor, we proposed that compounds with high membrane partitioning would result in increased values of k_{on}. We have extended these observations to include the β_1-adrenoceptor, comparing observed kinetic rate parameters with the degree of interaction with IAMs (K_{IAM}) and measures of lipophilicity (Log P and $logD_{7.4}$). As predicted the association rate of the compounds was seemingly directly influenced by their lipophilicity ($logD_{7.4}$); however, surprisingly the magnitude of interaction with the membrane surrounding the receptor, as determined through the artificial membrane partition coefficient (or K_{IAM}), did not further enhance this correlation.

In the previous study of the β_2-adrenoceptor, we hypothesized that the membrane itself could interact specifically with drugs,[20] through ionic and hydrogen-bonding interactions,[21] effectively concentrating drug molecules close to the surface of the membrane (relative to the bulk solution). In addition to the drug concentrating effect of the membrane, the loss of drug associated water,[3] and lateral diffusion across a two-dimensional cellular surface (rather than three dimensions in aqueous bulk) could all contribute to increased ligand-receptor association rates.[22] These rate enhancing effects may be applied not only to membrane-like structures (e.g., phospholipids) but also to the extracellular surfaces of the receptor

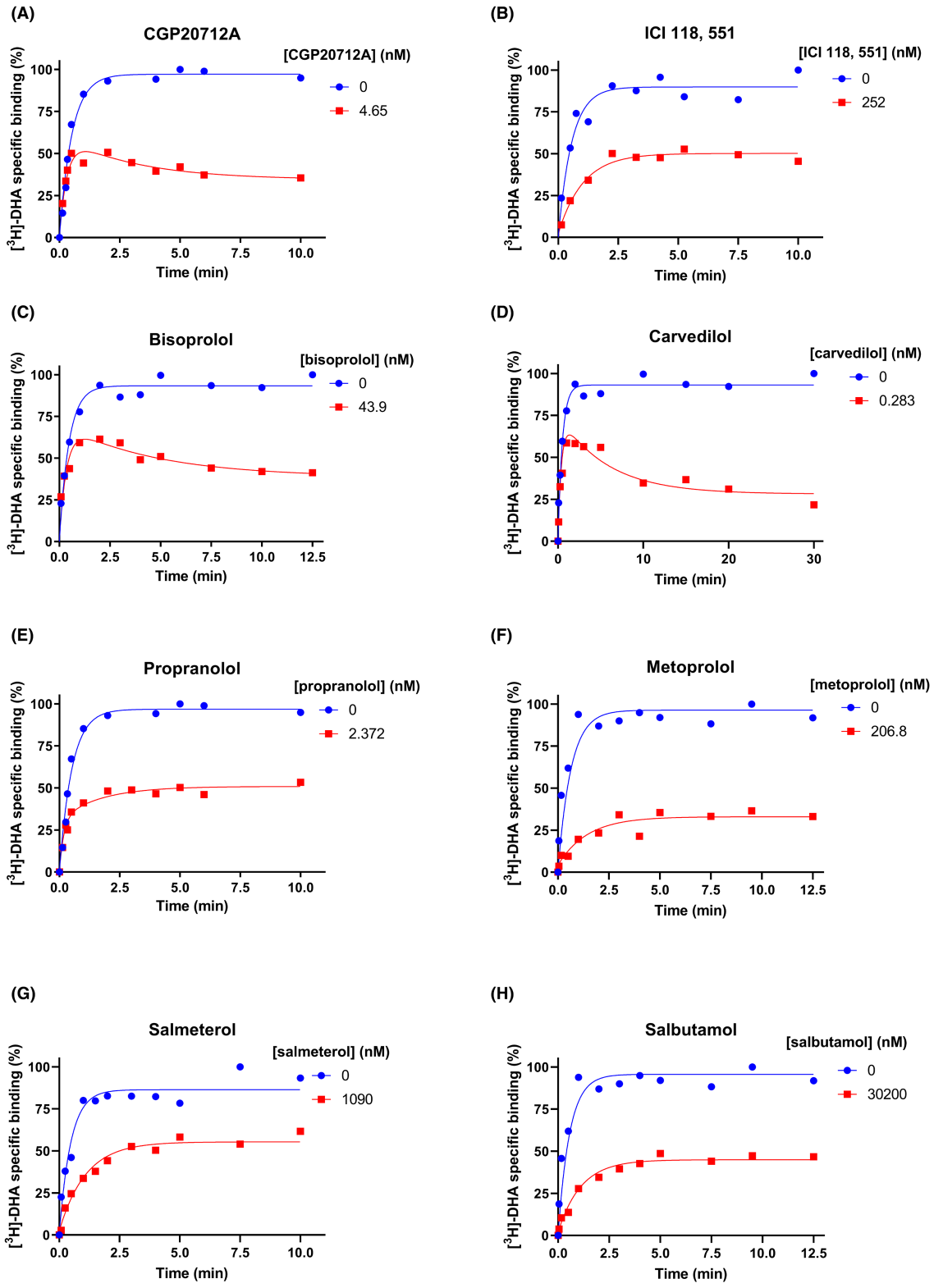

FIGURE 3 [^{3}H]-DHA competition kinetic curves in the presence of CGP20712A (A), ICI 118551(B), bisoprolol (C), carvedilol (D), propranolol (E), metoprolol (F), salmeterol, and (H) salbutamol. CHO-β_1 membranes were incubated with ~3 nM [^{3}H]-DHA and either 0-, 1-, 3-, 10- or 100-fold K_i of unlabeled competitor. Plates were incubated at 37°C for the indicated time points and NSB levels were determined in the presence of 1 μM propranolol. Data were fitted to the equations described in the Methods to calculate k_{on} and k_{off} values for the unlabelled ligands; these are summarized in Table 1. Data are presented as mean ± range from a representative of ≥3 experiments performed in singlet.

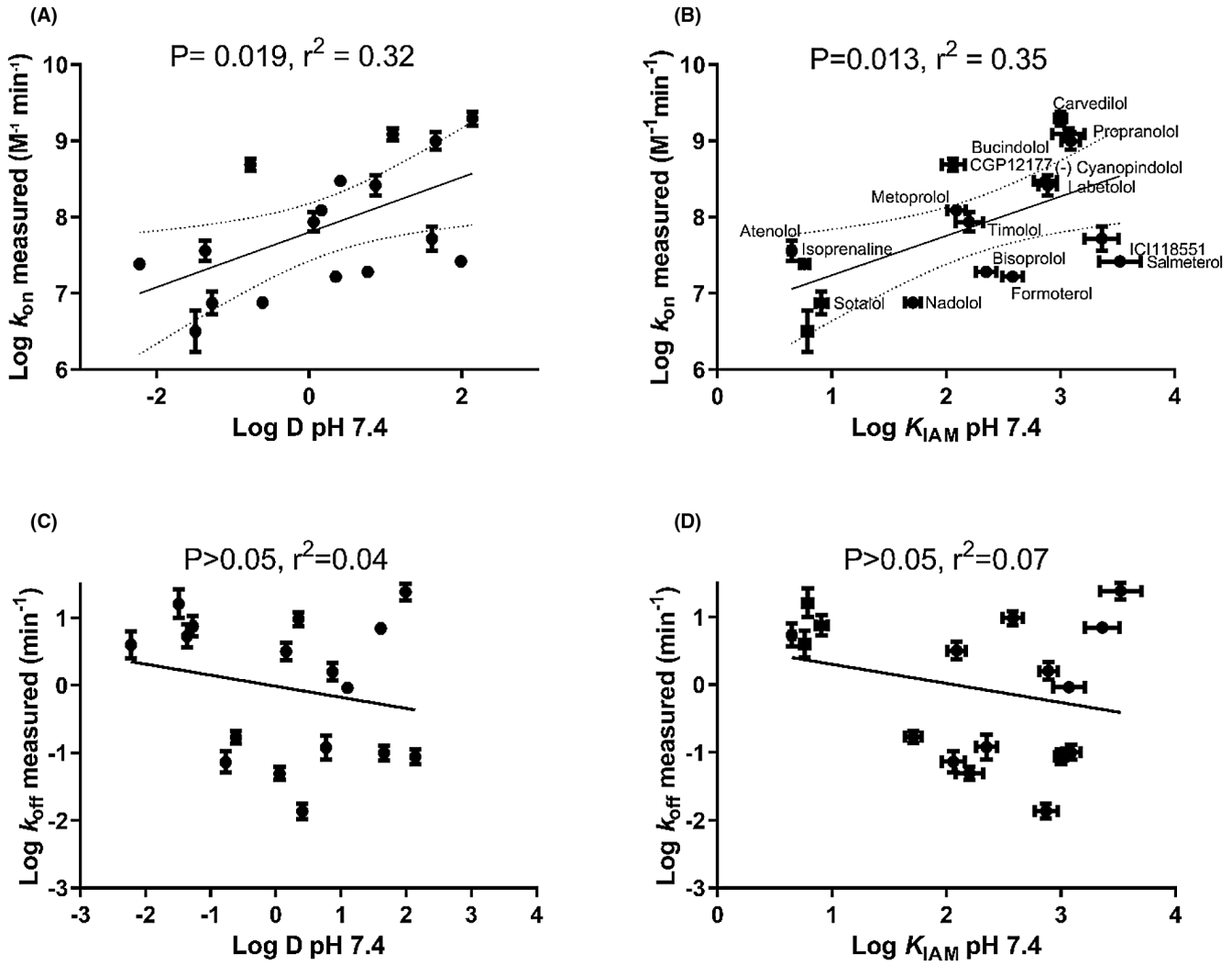

FIGURE 4 Correlating β_1 adrenoceptor ligand physiochemical parameters with kinetically derived parameters. Correlation plot showing the relationship between (A) log k_{on} and log $D_{7.4}$ and (B) log k_{on} and log $K_{IAM7.4.}$ Correlation plot showing the relationship between (C) log k_{off} and log $D_{7.4}$ and (D) log k_{off} and log $K_{IAM7.4}$. All data used in these plots are detailed in Table 1 with log $D_{7.4}$ and log $K_{IAM7.4}$ values from.[12] Data are presented as mean ± SEM from three or more experiments.

itself (e.g., amino acids with a polar, hydrophilic and a nonpolar, hydrophobic end). A compound can have the right physicochemical properties to facilitate a fast on-rate, but it must also have the right complementary structural features to facilitate its interaction with the receptors binding pocket.

Mutational, crystal modeling and docking studies have highlighted the key role that specific regions of these receptors forming the entrance to the binding pocket, play in dictating overall drug–receptor affinity[3,23,24,25,26,27,28,29] and kinetics.[10] A comparison of the residues of both β-adrenoceptor subtypes has suggested the importance of non-conserved electrostatic interactions as well as conserved aromatic contacts in the early steps of the binding process.[5,10] Similarly, on exit molecules have been shown to pause in what would now be termed the extracellular vestibule, a site 9–15 Å from the orthosteric binding site. These same sites have been shown to serve as secondary binding pockets during MD simulations of ligand entry.[3,4]

Based on the above, one plausible explanation for differences in drug–receptor subtype association rate stems from the different amino acid composition of their vestibular regions.[29-31] The extracellular vestibule of the β_2AR is well known to have a more extensive polar network.[10,32] In the β_2-adrenoceptor structure, the polar hydrophobic amino acid Tyr308$^{7.35\times34}$ contains an oxygen atom in the side chain, which is capable of acting as a H-bond donor or acceptor and has been postulated to form a key node in the pathway to successful ligand binding.[3] Superscript notation corresponds to the GPCRDB numbering.[33] Mutation of this residue to structurally equivalent phenylalanine found in the β_1-adrenoceptor structure (Phe259$^{7.35\times34}$), and a purely hydrophobic amino acid, has been shown to reduce the binding affinity of a wide range of β_2 adrenergic ligands firmly establishing its importance in the binding process.[23] The idea that specific residues (hydrophobic/charged) residues may guide lipophilic polar molecules into the orthosteric binding pocket, it is very much in line with

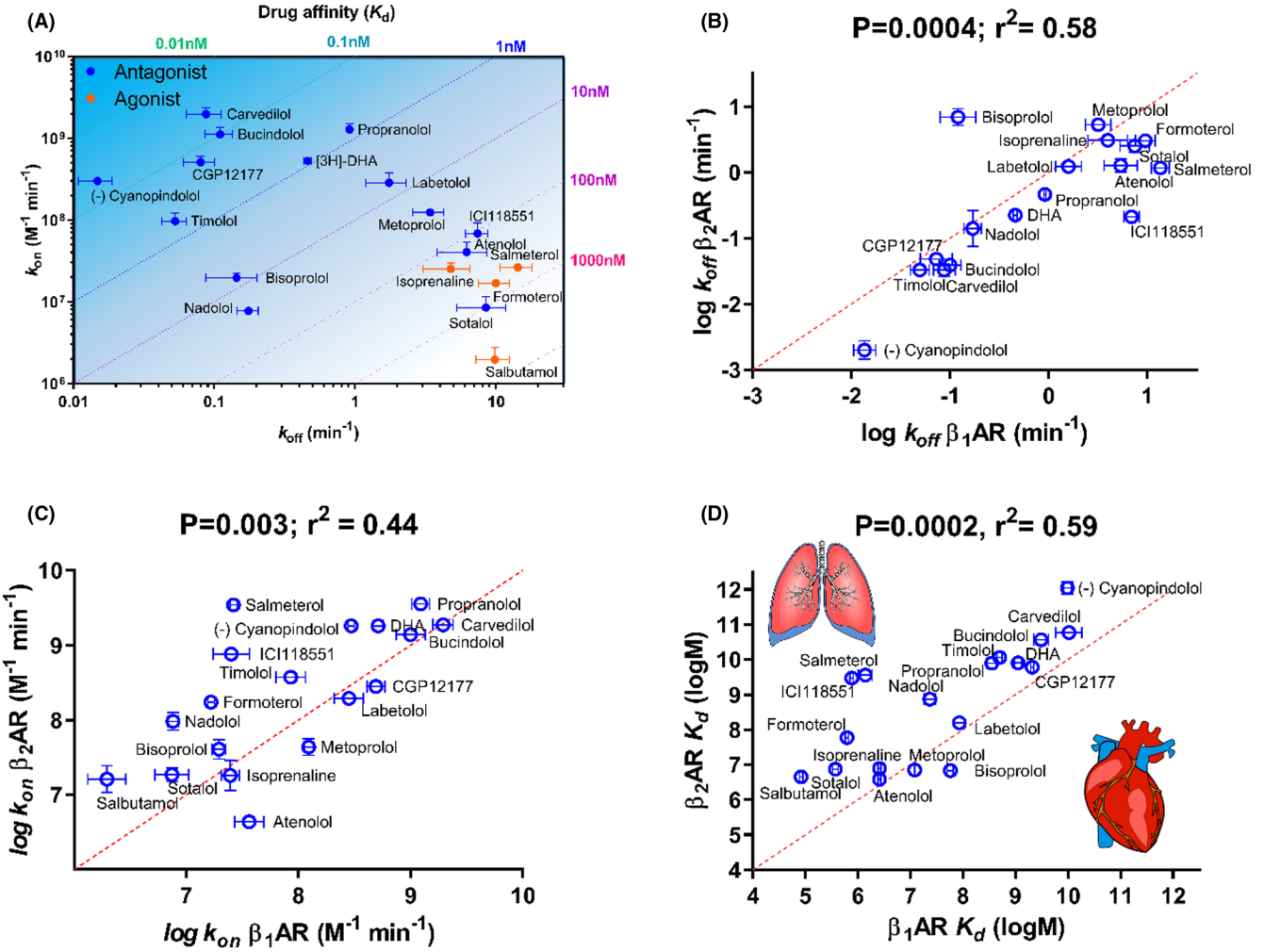

FIGURE 5 Summarizing the role of kinetics in dictating β_1-adrenoceptor affinity and selectivity. (A) Plot of β_1AR k_{off} versus β_1AR k_{on} values with affinity indicated by the diagonal dotted lines. (B) Plot of β_1AR k_{off} versus β_2AR k_{off} values. (C) Plot of β_1AR k_{on} versus β_2AR k_{on} values. (D) Plot of β_1AR log K_d versus β_2AR log K_d values. Kinetic values are presented as mean ± SEM from three or more experiments detailed in Table 1.

predictions from MD studies which highlight the probability of binding from different regions of the outer pocket.[3] This concept is also consistent with the idea that the receptor itself can influence local drug concentrations and in so doing directly dictate drug-receptor affinity through an increase in measured on-rate.[19] The relative differences in extracellular surface lipophilicity and polarity between the β_1 and β_2-adrenoceptor subtypes are summarized in Figure 7.

Ligand binding likely occurs in a multistage process: Initially, the membrane acts as a vehicle to concentrate drug molecules at the receptor surface contributing to the loss of ligand associated water molecules and allowing binding to proceed in several "smaller" steps, with lower energy barriers compared with a one-step mechanism, culminating in a more rapid binding process.[34,35] On reaching the vestibule further water loss occurs as drug interacts with specific amino acids, the strength of interaction being determined by a combination of hydrophobicity and polarity. Finally, drug enters the negatively charged binding pocket, this charge contributing to accelerated association.

It is reasonable to assume that the process of unbinding and binding follows a similar path but in opposite directions. A slower dissociation rate from the β_2- adrenoceptor could be partly caused by an extended residence time in the vestibule of receptor, the result of both the polar and hydrophobic interactions important in facilitating ligand association. This being the case the absence of key polar residue Tyr308$^{7.35\times34}$ in the β_1-adrenoceptor structure should result in an overall more rapid dissociation rate for key β_2-adrenoceptor specific ligands. This idea appears to be consistent with both the kinetic on and off-rates measured at these two receptor subtypes[6,9,12] and the reduced affinities observed for ligands following the Y308F mutation.[23] The relationship between association and dissociation rates for these ligands across these two receptor subtypes is shown in Figure S2.

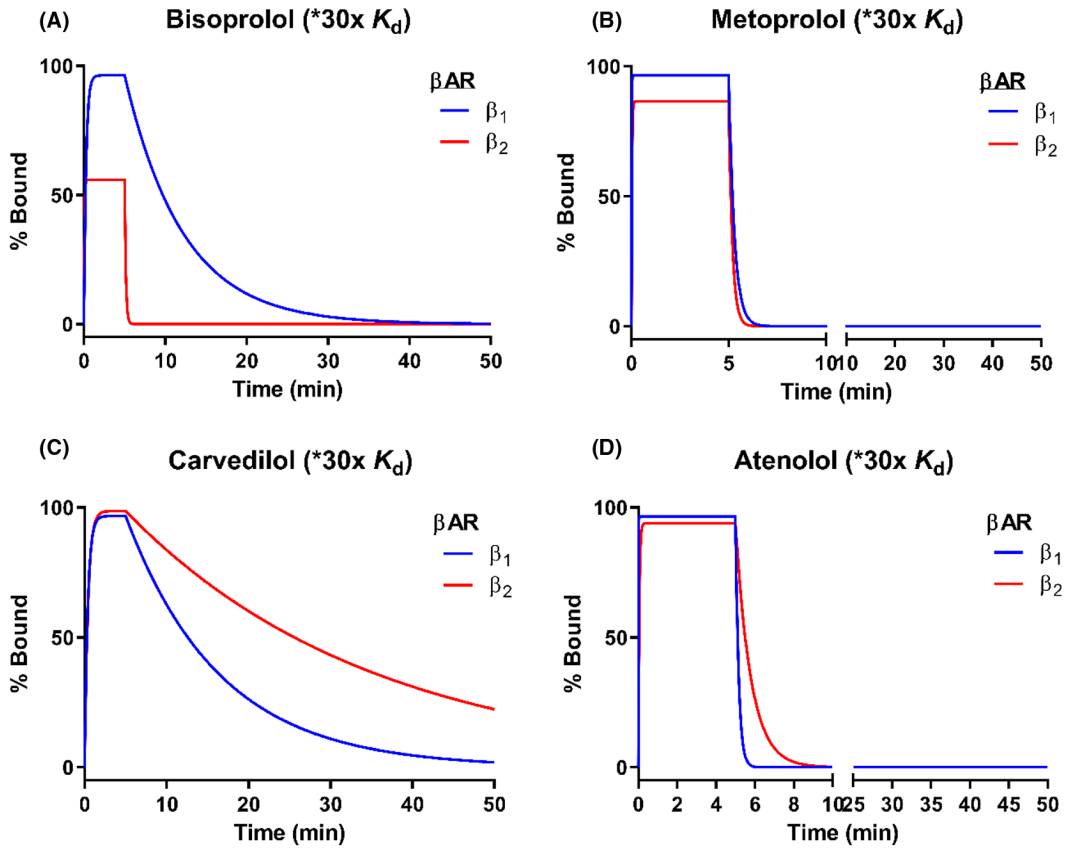

FIGURE 6 Summarizing the role of kinetics in dictating β_1-adrenoceptor selectivity. Modeling the association and dissociation of clinically relevant β-blockers. Simulated binding of clinically relevant β-blockers (A) bisoprolol (B) metoprolol (C) carvedilol and (D) atenolol to human β_1-adrenoceptors and β_2-adrenoceptors at concentrations 30 *K_d of the β_1-adrenoceptor. Dissociation occurs at 5 min point initiated by the removal of free ligand. The kinetic parameters used to construct these simulations are detailed in Table 1.

Kinetic selectivity is likely to be one of the key steps to reducing the side effect profile of β-adrenergic compounds. This tactic has proved to be effective in reducing the side effect profile of muscarinic M_3 antagonists which based on affinity values cannot be considered particularly selective for one receptor subtype over another.[6,7] In the current study, we are able for the first time to rationalize the improved affinity of bisoprolol for the β_1-adrenoceptor over the β_2-adrenoceptor which results from its much-reduced dissociation rate (50-fold, see Figures 5B and 6A).[12]

Bisoprolol's use in the clinic in patients with chronic heart failure and COPD is recognized as being associated with fewer side effects and potentially an improvement in mortality compared with the other β-blockers, a fact that could be rationalized based on its improved kinetic selectivity for the β_1-adrenoreceptors, cumulating in fewer off-target effects and characterized by its slow elimination and accumulation in the heart.[36-41] Other clinically used β-blockers include metoprolol and atenolol. However, based on the current data only atenolol can be considered marginally selective in terms of its overall affinity for β_1 and β_2-adrenoceptors. Neither drug can be considered kinetically selective in terms of their measured off-rates. Other non-selective β_2-adrenoceptor blockers such as carvedilol appear to be if anything more selective for β_2-adrenoreceptors over β_1-adrenoreceptors with repercussions for patients with underlying respiratory disease[42,43] where greater reductions in forced expiratory volume (lung function) have been observed[44-46] (see Figure 6).

Bisoprolol selective effects in the heart are clearly beneficial in the patients with heart and lung disease, but in terms of the treatment of heart failure, some reports suggest that carvedilol may produce equivalent or an improved overall reduced chance of all-cause mortality in systolic heart failure compared with other more selective agents such as bisoprolol.[47-54] Any number of factors could contribute to this including carvedilol's relatively slower dissociation from the β_1-adrenoreceptor or its vasodilatory alpha-receptor blocking effects.[53,55,56] Alternatively, its apparent kinetic selectivity for the β_2-adrenoreceptor, and/or biased signaling profile could potentially contribute to beneficial remodeling effects in the heart.[57,58]

In conclusion, we hope that the new kinetic data outlined in this study will reignite research into the discovery and development of kinetically selective ligands for the β_1-adrenoceptor, thereby reducing the overall burden of side effects associated with the use of β-blockers.

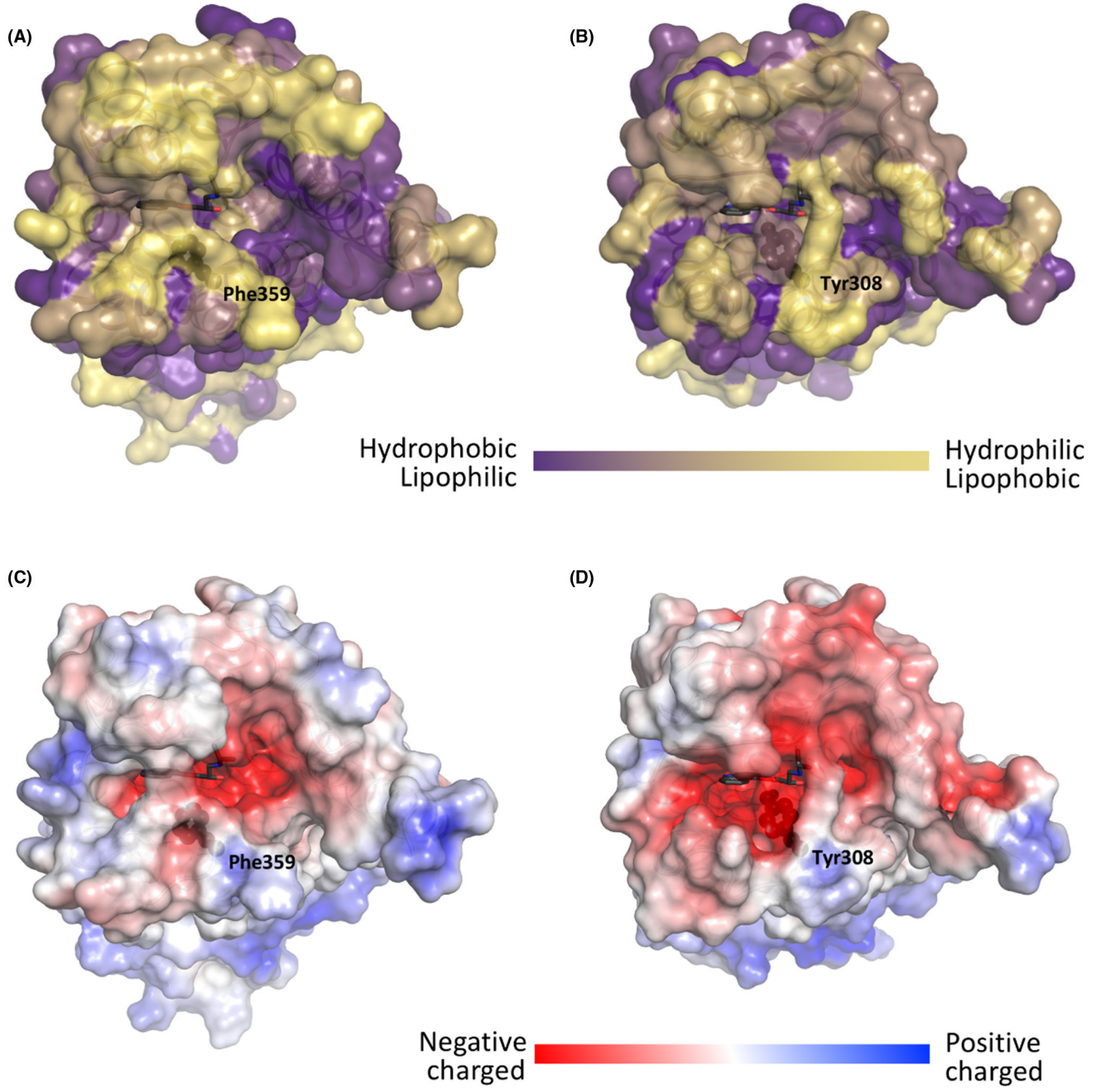

FIGURE 7 Comparison of the extracellular surfaces including vestibules and orthosteric pockets between the human β_1AR and β_2AR. Extracellular surface lipophilicity of the β_1AR and β_2AR is shown in (A) and (B) respectively. Extracellular surface polarity of the β_1AR and β_2AR is shown in (C) and (D) respectively. Overall, the surface of the β_2AR is dominated by more negatively charged patches and its hydrophobic regions are more numerous and widely spread. Diffusion in 2D allows lipophilic charged molecules to rapidly reach their target receptor through a reduction in dimensionality. On entering the outer vestibule drug interacts with specific residues which further loosens associated water molecules and contributes to accelerated association rates. For example, within the β_2-adrenoceptor structure certain basic drug molecules form a loose interaction with the more numerous polar amino acid residues eg. Tyr308$^{7.35\times34}$ (Y), thereby increasing the probability of a successful drug binding event. Finally, as a ligand enters the negatively charged binding pocket the positive charge of the ligands contributes to their rapid association with the orthosteric binding site.

AUTHOR CONTRIBUTIONS

Participated in research design: Sykes, Charlton, Veprintsev. Conducted experiments: Sykes, Reilly, Jiménez-Rosés. Performed data analysis: Sykes, Jiménez-Rosés, Reilly. Wrote or contributed to writing on manuscript: Sykes, Charlton, Jiménez-Rosés, Veprintsev, Reilly, Fairhurst.

FUNDING INFORMATION

This study was financed by Novartis Institutes for Biomedical Research.

ACKNOWLEDGMENT

Open access funding enabled and organized by ProjektDEAL.

CONFLICT OF INTEREST

SJC is a founder of Excellerate Bioscience Ltd., a CRO. DAS and DBV are both founders of Z7 Biotech Ltd a CRO. The remaining authors declare that the research was conducted in the absence of any commercial or financial relationships that could be construed as a potential conflict of interest.

ETHICS STATEMENT

No animals, human tissue, human volunteers, or patients were used in this stud.

DATA AVAILABILITY STATEMENT

The data that support the findings of this study are available from the corresponding author upon reasonable request. Some data may not be made available because of privacy or ethical restrictions.

ORCID

David A. Sykes https://orcid.org/0000-0002-6606-888X
Mireia Jiménez-Rosés https://orcid.org/0000-0002-4049-8670
Steven J. Charlton https://orcid.org/0000-0001-8841-2752
Dmitry B. Veprintsev https://orcid.org/0000-0002-3583-5409

REFERENCES

1. Harries AD. Beta-blockade in asthma. *Br Med J (Clin Res ed)*. 1981;282:1321.
2. Harrington J. Cardiac-specific beta-blockers and asthma: an end to fear? *Respirology*. 2020;26:216-217.
3. Dror RO, Pan AC, Arlow DH, et al. Pathway and mechanism of drug binding to G-protein-coupled receptors. *Proc Natl Acad Sci USA*. 2011;108:13118-13123.
4. Gonzalez A, Perez-Acle T, Pardo L, Deupi X. Molecular basis of ligand dissociation in beta-adrenergic receptors. *PLoS One*. 2011;6:e23815.
5. Selvam B, Wereszczynski J, Tikhonova IG. Comparison of dynamics of extracellular accesses to the beta(1) and beta(2) adrenoceptors binding sites uncovers the potential of kinetic basis of antagonist selectivity. *Chem Biol Drug des*. 2012;80:215-226.
6. Sykes DA, Dowling MR, Leighton-Davies J, et al. The influence of receptor kinetics on the onset and duration of action and the therapeutic index of NVA237 and tiotropium. *J Pharmacol Exp Ther*. 2012;343:520-528.
7. Tautermann CS, Kiechle T, Seeliger D, et al. Molecular basis for the long duration of action and kinetic selectivity of tiotropium for the muscarinic M3 receptor. *J Med Chem*. 2013;56:8746-8756.
8. Boursier ME, Levin S, Zimmerman K, et al. The luminescent HiBiT peptide enables selective quantitation of G protein-coupled receptor ligand engagement and internalization in living cells. *J Biol Chem*. 2020;295:5124-5135.
9. Ramos I, Aparici M, Letosa M, et al. Abediterol (LAS100977), an inhaled long-acting beta2-adrenoceptor agonist, has a fast association rate and long residence time at receptor. *Eur J Pharmacol*. 2018;819:89-97.
10. Xu X, Kaindl J, Clark MJ, et al. Binding pathway determines norepinephrine selectivity for the human beta1AR over beta2AR. *Cell Res*. 2020;31:569-579.
11. Sykes DA, Charlton SJ. Slow receptor dissociation is not a key factor in the duration of action of inhaled long-acting beta2-adrenoceptor agonists. *Br J Pharmacol*. 2012;165:2672-2683.
12. Sykes DA, Parry C, Reilly J, Wright P, Fairhurst RA, Charlton SJ. Observed drug-receptor association rates are governed by membrane affinity: the importance of establishing "micro-pharmacokinetic/pharmacodynamic relationships" at the beta2-adrenoceptor. *Mol Pharmacol*. 2014;85:608-617.
13. Carter CM, Leighton-Davies JR, Charlton SJ. Miniaturized receptor binding assays: complications arising from ligand depletion. *J Biomol Screen*. 2007;12:255-266.
14. Motulsky HJ, Mahan LC. The kinetics of competitive radioligand binding predicted by the law of mass action. *Mol Pharmacol*. 1984;25:1-9.
15. Cheng Y, Prusoff WH. Relationship between the inhibition constant (K1) and the concentration of inhibitor which causes 50 per cent inhibition (I50) of an enzymatic reaction. *Biochem Pharmacol*. 1973;22(23):3099–3108.
16. Staus DP, Strachan RT, Manglik A, et al. Allosteric nanobodies reveal the dynamic range and diverse mechanisms of G-protein-coupled receptor activation. *Nature*. 2016;535:448-452.
17. Liu H, Carter GT, Tischler M. Immobilized artificial membrane chromatography with mass spectrometric detection: a rapid method for screening drug-membrane interactions. *Rapid Commun Mass Spectrom*. 2001;15:1533-1538.
18. Vrakas D, Giaginis C, Tsantili-Kakoulidou A. Electrostatic interactions and ionization effect in immobilized artificial membrane retention. A comparative study with octanol-water partitioning. *J Chromatogr A*. 2008;1187:67-78.
19. Gherbi K, Briddon SJ, Charlton SJ. Micro-pharmacokinetics: quantifying local drug concentration at live cell membranes. *Sci Rep*. 2018;8:3479.
20. Sargent DF, Schwyzer R. Membrane lipid phase as catalyst for peptide-receptor interactions. *Proc Natl Acad Sci USA*. 1986;83:5774-5778.
21. Avdeef A, Box KJ, Comer JE, Hibbert C, Tam KY. pH-metric logP 10. Determination of liposomal membrane-water partition coefficients of ionizable drugs. *Pharm Res*. 1998;15:209-215.
22. McCloskey MA, Poo MM. Rates of membrane-associated reactions: reduction of dimensionality revisited. *J Cell Biol*. 1986;102:88-96.
23. Baker JG. The selectivity of beta-adrenoceptor antagonists at the human beta1, beta2 and beta3 adrenoceptors. *Br J Pharmacol*. 2005;144:317-322.
24. Isogaya M, Sugimoto Y, Tanimura R, et al. Binding pockets of the beta(1)- and beta(2)-adrenergic receptors for subtype-selective agonists. *Mol Pharmacol*. 1999;56:875-885.
25. Kaszuba K, Rog T, Bryl K, Vattulainen I, Karttunen M. Molecular dynamics simulations reveal fundamental role of water as factor determining affinity of binding of beta-blocker nebivolol to beta(2)-adrenergic receptor. *J Phys Chem B*. 2010;114:8374-8386.
26. Kikkawa H, Isogaya M, Nagao T, Kurose H. The role of the seventh transmembrane region in high affinity binding of a beta 2-selective agonist TA-2005. *Mol Pharmacol*. 1998;53:128-134.
27. Plazinska A, Kolinski M, Wainer IW, Jozwiak K. Molecular interactions between fenoterol stereoisomers and derivatives and the beta(2)-adrenergic receptor binding site studied by docking and molecular dynamics simulations. *J Mol Model*. 2013;19:4919-4930.
28. Plazinska A, Plazinski W, Jozwiak K. Agonist binding by the beta2-adrenergic receptor: an effect of receptor conformation on ligand association-dissociation characteristics. *Eur Biophys J*. 2015;44:149-163.

29. Warne T, Serrano-Vega MJ, Baker JG, et al. Structure of a beta1-adrenergic G-protein-coupled receptor. *Nature*. 2008;454:486-491.
30. Masureel M, Zou Y, Picard LP, et al. Structural insights into binding specificity, efficacy and bias of a beta2AR partial agonist. *Nat Chem Biol*. 2018;14:1059-1066.
31. Vanni S, Neri M, Tavernelli I, Rothlisberger U. Observation of "ionic lock" formation in molecular dynamics simulations of wild-type beta 1 and beta 2 adrenergic receptors. *Biochemistry*. 2009;48:4789-4797.
32. Ring AM, Manglik A, Kruse AC, et al. Adrenaline-activated structure of beta2-adrenoceptor stabilized by an engineered nanobody. *Nature*. 2013;502:575-579.
33. Isberg V, Mordalski S, Munk C, et al. GPCRdb: an information system for G protein-coupled receptors. *Nucleic Acids Res*. 2016;44:D356-D364.
34. AP IJ, Guo D. Drug-target association kinetics in drug discovery. *Trends Biochem Sci*. 2019;44:861-871.
35. Vauquelin G. Cell membranes… and how long drugs may exert beneficial pharmacological activity in vivo. *Br J Clin Pharmacol*. 2016;82:673-682.
36. Kang J, More KN, Pyo A, Jung Y, Kim DY, Chang DJ. Bisoprolol-based (18)F-PET tracer: synthesis and preliminary in vivo validation of beta1-blocker selectivity for beta1-adrenergic receptors in the heart. *Bioorg Med Chem Lett*. 2021;36:127789.
37. Kubota Y, Asai K, Furuse E, et al. Impact of beta-blocker selectivity on long-term outcomes in congestive heart failure patients with chronic obstructive pulmonary disease. *Int J Chron Obstruct Pulmon Dis*. 2015;10:515-523.
38. Liao KM, Lin TY, Huang YB, Kuo CC, Chen CY. The evaluation of beta-adrenoceptor blocking agents in patients with COPD and congestive heart failure: a nationwide study. *Int J Chron Obstruct Pulmon Dis*. 2017;12:2573-2581.
39. Su VY, Chang YS, Hu YW, et al. Carvedilol, bisoprolol, and metoprolol use in patients with coexistent heart failure and chronic obstructive pulmonary disease. *Medicine (Baltimore)*. 2016;95:e2427.
40. Lainscak M, Podbregar M, Kovacic D, Rozman J, von Haehling S. Differences between bisoprolol and carvedilol in patients with chronic heart failure and chronic obstructive pulmonary disease: a randomized trial. *Respir Med*. 2011;105(Suppl 1):S44–S49.
41. Taniguchi T, Ohtani T, Mizote I, et al. Switching from carvedilol to bisoprolol ameliorates adverse effects in heart failure patients with dizziness or hypotension. *J Cardiol*. 2013;61:417-422.
42. Baker JG, Wilcox RG. Beta-blockers, heart disease and COPD: current controversies and uncertainties. *Thorax*. 2017;72:271-276.
43. Benson MK, Berrill WT, Cruickshank JM, Sterling GS. A comparison of four beta-adrenoceptor antagonists in patients with asthma. *Br J Clin Pharmacol*. 1978;5:415-419.
44. Dungen HD, Apostolovic S, Inkrot S, et al. Titration to target dose of bisoprolol vs. carvedilol in elderly patients with heart failure: the CIBIS-ELD trial. *Eur J Heart Fail*. 2011;13:670-680.
45. Jabbal S, Anderson W, Short P, Morrison A, Manoharan A, Lipworth BJ. Cardiopulmonary interactions with beta-blockers and inhaled therapy in COPD. *QJM*. 2017;110:785-792.
46. Jabbour A, Macdonald PS, Keogh AM, et al. Differences between beta-blockers in patients with chronic heart failure and chronic obstructive pulmonary disease: a randomized crossover trial. *J Am Coll Cardiol*. 2010;55:1780-1787.
47. Bølling R, Scheller NM, Køber L, Poulsen HE, Gislason GH, Torp-Pedersen C. Comparison of the clinical outcome of different beta-blockers in heart failure patients: a retrospective nationwide cohort study. *Eur J Heart Fail*. 2014;16:678-684.
48. Choi KH, Lee GY, Choi JO, et al. The mortality benefit of carvedilol versus bisoprolol in patients with heart failure with reduced ejection fraction. *Korean J Intern Med*. 2019;34:1030-1039.
49. DiNicolantonio JJ, Lavie CJ, Fares H, Menezes AR, O'Keefe JH. Meta-analysis of carvedilol versus beta 1 selective beta-blockers (atenolol, bisoprolol, metoprolol, and nebivolol). *Am J Cardiol*. 2013;111:765-769.
50. Hart SM. Influence of beta-blockers on mortality in chronic heart failure. *Ann Pharmacother*. 2000;34:1440-1451.
51. Hulkower S, Aiken BA, Stigleman S. Clinical inquiry: what is the best beta-blocker for systolic heart failure? *J Fam Pract*. 2015;64:122-123.
52. Rain C, Rada G. Is carvedilol better than other beta-blockers for heart failure? *Medwave*. 2015;15(Suppl 1):e6168.
53. Remme WJ. Which beta-blocker is most effective in heart failure? *Cardiovasc Drugs Ther*. 2010;24:351-358.
54. Wikstrand J, Wedel H, Castagno D, McMurray JJ. The large-scale placebo-controlled beta-blocker studies in systolic heart failure revisited: results from CIBIS-II, COPERNICUS and SENIORS-SHF compared with stratified subsets from MERIT-HF. *J Intern Med*. 2014;275:134-143.
55. Metra M, Cas LD, di Lenarda A, Poole-Wilson P. Beta-blockers in heart failure: are pharmacological differences clinically important? *Heart Fail Rev*. 2004;9:123-130.
56. Weir RA, Dargie HJ. Carvedilol in chronic heart failure: past, present and future. *Future Cardiol*. 2005;1:723-734.
57. Kim IM, Wang Y, Park KM, et al. Beta-arrestin1-biased beta1-adrenergic receptor signaling regulates microRNA processing. *Circ Res*. 2014;114:833-844.
58. Wisler JW, DeWire SM, Whalen EJ, et al. A unique mechanism of beta-blocker action: carvedilol stimulates beta-arrestin signaling. *Proc Natl Acad Sci USA*. 2007;104:16657-16662.

SUPPORTING INFORMATION

Additional supporting information can be found online in the Supporting Information section at the end of this article.

How to cite this article: Sykes DA, Jiménez-Rosés M, Reilly J, Fairhurst RA, Charlton SJ, Veprintsev DB. Exploring the kinetic selectivity of drugs targeting the β_1-adrenoceptor. *Pharmacol Res Perspect*. 2022;10:e00978. doi: 10.1002/prp2.978